

Matrix metalloproteinase-1 expression is regulated by HIF-1-dependent and epigenetic mechanisms and serves a tumor-suppressive role in gastric cancer progression

KOTARO ITO¹, YOSHIHIKO KITAJIMA², KEITA KAI³, SHOHEI MATSUFUJI¹, KOHEI YAMADA¹, NORIYUKI EGAWA¹, HIROSHI KITAGAWA¹, KEIICHIRO OKUYAMA¹, TOMOKAZU TANAKA¹ and HIROKAZU NOSHIRO¹

¹Department of Surgery, Saga University Faculty of Medicine, Saga 849-8501;

²Department of Surgery, National Hospital Organization Higashisaga Hospital, Miyaki, Saga 849-0101; ³Department of Pathology, Saga University Hospital, Saga 849-8501, Japan

Received June 18, 2021; Accepted October 11, 2021

DOI: 10.3892/ijo.2021.5282

Abstract. The matrix metalloproteinase (MMP) family is associated with degradation of the extracellular matrix and is known to promote cancer invasion. The present study aimed to investigate the biological role of MMP-1 in gastric cancer cells and analyze the association between MMP-1 expression and the clinical outcomes of gastric cancer patients. In the present study, hypoxia accelerated invasion, accompanied by elevated MMP-1 expression in the gastric cancer cell line 58As9. Additionally, hypoxia-inducible factor-1 α (HIF-1 α) knockdown in 58As9 cells reduced MMP-1 expression under hypoxic conditions. Treatment with 5-aza-2-deoxycytidine and trichostatin A restored MMP-1 expression in the MMP-1-deficient cell lines MKN45 and MKN74. These results indicated that MMP-1 expression was controlled by both HIF-1 α -dependent and epigenetic mechanisms in gastric cancer cell lines. In

addition, MMP-1 knockdown impaired the hypoxia-induced invasiveness of 58As9 cells, implicating MMP-1 in the elevated invasion. By contrast, knockdown enhanced the proliferative ability of 58As9 cells, whereby expression of cell cycle-related genes was subsequently altered. In nude mouse models, the knockdown accelerated the growth of xenograft tumor and the development of peritoneal dissemination. In an immunohistochemical study using 161 surgically resected cancer tissues, the Ki67 score was significantly higher in the group with low MMP-1 expression ($P < 0.001$). Disease-free survival (DFS) and disease-specific survival (DSS) were both significantly reduced in patients with low MMP-1 expression (log-rank test; DFS: $P = 0.005$; DSS: $P = 0.022$). Multivariate analysis demonstrated that MMP-1 expression was an independent prognostic factor for DFS and DSS [DFS: HR=2.11 (1.22-3.92) $P = 0.005$, DSS: HR=2.90 (1.23-8.50) $P = 0.012$]. In conclusion, the present study indicated that MMP-1 may serve as a tumor-suppressive factor that inhibits gastric cancer progression, although it promoted invasion *in vitro*.

Correspondence to: Dr Kotaro Ito, Department of Surgery, Saga University Faculty of Medicine, 5-1-1 Nabeshima, Saga 849-8501, Japan

E-mail: sh2806@cc.saga-u.ac.jp

Abbreviations: ACTB, β -actin; AMFR, autocrine motility factor receptor; C-MET, c-Mesenchymal-epithelial transition factor; DFS, disease-free survival; DSS, disease-specific survival; GC, gastric cancer; HIF-1 α , hypoxia-inducible factor-1 α ; IHC, immunohistochemistry; LOXL2, lysyl oxidase-like 2; Ly, lymphatic invasion; MMP, matrix metalloproteinase; N, lymph node metastasis; RHOA, Ras homolog family member A; ROCK1, ρ -associated protein kinase 1; RT-qPCR, reverse-transcription quantitative polymerase chain reaction; SC, scramble; T, tumor depth; TSA, Trichostatin A; WB, western blotting; UPAR, urokinase-type plasminogen activator receptor; V, vascular invasion; 5-aza-dC, 5-Aza-2-deoxycytidine

Key words: matrix metalloproteinase, gastric cancer, hypoxia, hypoxia inducible factor, epigenetic, proliferation, invasion

Introduction

Despite significant advances in the prevention and treatment of gastric cancer (GC) over the past few decades, there are ~1 million new cases annually, making GC the fifth most diagnosed cancer worldwide (1). The etiology of this disease is multifactorial and includes the combination of genetic predisposition and environmental factors (2). GC still has a poor prognosis due to metastasis. To develop more effective therapies for advanced GC, there is a need to clarify the biological mechanism behind this disease.

Although the development of molecular biology has gradually deepened our understanding of GC, the molecular mechanisms underlying its progression remain to be elucidated. There is thus an urgent need to identify biomarkers that could potentially serve as therapeutic targets or prognostic indicators in patients with GC.

Similar to other solid tumors, GC causes widespread hypoxia. Previous reports have shown that hypoxia is an

important microenvironmental factor in the promotion of tumor progression (3,4). Hypoxia-inducible factor-1 (HIF-1) is a heterodimeric transcription factor composed of a constitutively expressed HIF-1 β subunit and an O₂ level-regulated HIF-1 α subunit (5,6). HIF-1 α is a well-known master regulator of invasion and metastasis in solid tumors, including GC, via its upregulation of target genes under hypoxia (7-12). In xenograft tumors, the manipulation of HIF-1 α activity by genetic or pharmacological methods has a significant effect on tumor growth via changes in angiogenesis, glucose metabolism and cell survival (13-16).

Matrix metalloproteinases (MMPs), a large family of zinc-containing endopeptidases composed of 25 members (including collagenase, gelatinase and stromelysin), are involved in the tissue remodeling and degradation of the extracellular matrix (17,18). The role of MMPs in cancer progression is attributed to their ability to degrade the extracellular matrix (19,20). Recent studies have revealed that MMPs also degrade several other biopolymers (21). MMP-1, also known as collagenase-1, specifically degrades interstitial collagen I, II and III and serves an important role in tumor cell progression and metastasis (22). High MMP1 expression has been identified in various types of cancer and is involved in the incidence or invasion of cancers (23-34). Several reports have shown that the increased expression of MMP-1 in different cancers is associated with unfavorable clinical outcomes, but the relationship between MMP-1 levels and patient outcomes in GC remains unclear (34-45).

The present study analyzed three GC cell lines: 58As9, MKN45 and MKN74. The 58As9 cell line exhibits hypoxia-induced cancer invasion, whereas the other two GC cell lines show limited invasiveness. MMP-1 was focused on as a candidate for regulating 58As9 cell invasion because of its hypoxia-dependent expression. Cells with knockdown of HIF-1 α and MMP-1 were analyzed to evaluate whether MMP-1 was responsible for the hypoxia-induced invasiveness of 58As9 cells and it was determined whether MMP-1 was an HIF-1 α target gene. The effect of MMP-1 knockdown was further investigated not only on cell proliferation *in vitro*, but also on tumor growth and the development of peritoneal dissemination in nude mice. Finally, MMP-1 expression in 161 surgically resected GC tissues was evaluated by immunohistochemistry (IHC) and the correlation between MMP-1 levels and clinical outcomes in GC patients was assessed. In this way, the present study aimed to clarify the role of MMP-1 expression in GC progression.

Materials and methods

Cell culture. The human GC cell lines 58As9, MKN45 and MKN74 were investigated. The 58As9 cell line was provided by the National Cancer Institute, Tokyo, Japan. MKN45 and MKN74 cells were purchased from RIKEN BRC cell bank. The characteristics of the cell lines are as follows: 58As9, signet-ring cell carcinoma; MKN45, poorly differentiated adenocarcinoma; and MKN74, moderately differentiated adenocarcinoma. The cell lines were grown in complete culture medium [RPMI-1640 medium (Sigma-Aldrich; Merck KGaA) supplemented with 10% fetal bovine serum (Biowest S.A.S.) and 100 μ g/ml kanamycin (Meiji Seika Kaisha, Ltd.)] at 37°C

in a humidified atmosphere and maintained under conditions of either normoxia (20% O₂ and 5% CO₂ air) or hypoxia (1% O₂, 5% CO₂ and 94% N₂).

Invasion assay. GC cells were resuspended in serum-free RPMI-1640 culture medium (1x10⁵ cells/500 μ l) and seeded onto the upper chambers of BioCoat Matrigel Invasion Chambers (cat. no. 354480; Corning, Inc.) in 24-well plates. Next, 750 μ l aliquots of the supernatant from cultures of MRC5 normal diploid fibroblasts were placed on the bottom chambers. Plates were incubated at 37°C for 24 h and then the non-invaded cells on the upper side of the filter were gently removed with a cotton swab. The invaded cells on the lower side of the filter were fixed in 4% paraformaldehyde for 15 min at room temperature and then stained with a 0.1% crystal violet solution for 15 min at room temperature. Using a light microscope, cells in three random fields were visualized and counted with ImageJ software v1.53 (National Institutes of Health). All experiments were performed in triplicate.

Western blotting (WB). Whole-cell lysates from cultured cells and xenograft tumors in mice were prepared by the resuspension of cells in lysis buffer [150 mM NaCl, 50 mM Tris-HCl, pH 7.5, 2 mM EDTA, 1% Triton X-100, 1% sodium deoxycholate, 2% sodium dodecyl sulfate, 28 μ M phenylmethylsulfonyl fluoride and a protease inhibitor cocktail mix (Roche Diagnostics GmbH)].

For WB analysis, the protein concentration was determined using Protein Assay Dye Reagent (cat. no. 5000006JA; Bio-Rad Laboratories, Inc.) according to the manufacturer's instructions. The samples were dissolved in NuPage LDS sample buffer (Invitrogen; Thermo Fisher Scientific, Inc.) and 1 M dithiothreitol and then heated for 5 min at 95°C. Briefly, 30 μ g of protein was separated on 5-20% Bis-Tris gels (Inter-Techno Co., Ltd.) and transferred to Hybond-ECL membranes (GE Healthcare; Cytiva). Membranes were blocked with 5% skimmed milk at room temperature for 30 min, and then incubated overnight at 4°C with the following primary antibodies: Anti-MMP-1 (1:5,000; cat. no. 134184; Abcam), anti-HIF-1 α (1:1,000; BD Biosciences), anti-CDK2 (1:1,000; cat. no. 32147; Abcam), anti-CDK6 (1:50,000; cat. no. 124821; Abcam), anti-cyclin B1 (1:2,000; cat. no. 181593; Abcam), anti-cyclin D1 (1:10,000; cat. no. 134175; Abcam), anti-p21 (1:1,000; cat. no. 109199; Abcam), anti-p27 KIP1 (1:5,000; cat. no. 32034; Abcam) and anti- β -actin (1:10,000, cat. no. AC15; Sigma-Aldrich; Merck KGaA). Membranes were then washed and incubated with the corresponding secondary antibodies (Goat Anti-Rabbit IgG; 1:5,000; cat. no. 4050-05; and Goat Anti-Mouse IgG, 1:5,000; cat. no. 1031-05; both SouthernBiotech) for 30 min at room temperature and the signal was developed using ECL Prime Western Blotting Detection Reagent (GE Healthcare; Cytiva). Images were acquired using a FUSION-FX7 imaging system (Vilber-Lourmat). Densitometry was performed using Bio-1D software v15.08 (Vilber-Lourmat).

Extraction of RNA and reverse-transcription quantitative (RT-q)PCR analysis. Cells were plated in 60 mm dishes and allowed to grow to 60-70% confluence. Total RNA was extracted as previously described (46). Total RNA was extracted from cell lines using an Isogen RNA extraction

kit (Nippon Gene Co., Ltd.) according to the manufacturer's protocol. RNA was converted into cDNA using a ReverTra Ace (Toyobo Life Science) reverse transcription reaction kit according to the manufacturer's protocol. RNA quantity and quality were measured with a NanoDrop ND-1000 spectrophotometer (NanoDrop Technologies; Thermo Fisher Scientific, Inc.). RT-qPCR was performed using the CFX Connect Real-Time PCR Detection System (Bio-Rad Laboratories, Inc.) with SsoAdvanced Universal SYBR Green Supermix (Bio-Rad Laboratories, Inc.) according to the manufacturer's protocol. After performing a denaturation step at 95°C for 3 min, PCR amplification was conducted with 50 cycles composed of denaturation for 15 sec at 95°C, annealing for 5 sec at 60°C and extension for 10 sec at 72°C. Expression of the gene of interest was normalized to β -actin (ACTB) mRNA levels by $2^{-\Delta\Delta C_q}$ method (47). The following primers were used: MMP-1: 5'-TCCCAAATCCTGTCCAGCC-3' (forward) 5'-CCGGACTTCATCTCTGTCCGG-3' (reverse); Ras homolog family member A (RHOA): 5'-GGTGATGGA GCCTGTGAAA-3' (forward) 5'-TGTGTCCCACAAAGC CAACT-3' (reverse); S100A4: 5'-ACAGATGAAGCTGCT TTCCAGA-3' (forward) 5'-TTCTTCCCTGGGCTGCTTA TCTG-3' (reverse); ρ -associated protein kinase 1 (ROCK1): 5'-CGAACCCCTAAAACACAGGCTG-3' (forward) 5'-CTT GGTGAGTTCCAGTTGCAG-3' (reverse); urokinase-type plasminogen activator receptor (UPAR): 5'-TAAGACCAA CGGGGATTGCC-3' (forward) 5'-AGGCTGGTGATC TTCAAGCC-3' (reverse); MMP-14: 5'-GGCTGCCTACCG ACAAGATT-3' (forward) 5'-GGGAGACTCAGGGATCCC TT-3' (reverse); lysyl oxidase-like 2 (LOXL2): 5'-AAGACC TGGAAGCAGATCTGTG-3' (forward) 5'-ATTCTTCAT GGGGTCCAGTGAC-3' (reverse); autocrine motility factor receptor (AMFR): 5'-CTGCATGTTGGACAGGAGGT-3' (forward) 5'-GAGGTGCAACGTCGAATTCG-3' (reverse); c-Mesenchymal-epithelial transition factor (C-MET): 5'-CCA GTGAAGTGGATGGCTTT-3' (forward) 5'-ATATCCGGG ACACCAGTTCA-3' (reverse); MMP-7: 5'-GCAAAGAGA TCCCCTGCAT-3' (forward) 5'-CCAGCGTTCATCCTC ATCGA-3' (reverse); ACTB: 5'-ACGCTCTGGCCGTA CCACT-3' (forward) 5'-TAATGTCACGCACGATTTCCC-3' (reverse). All experiments were performed in triplicate and independently repeated at least three times.

RNA interference. Cells were plated in 6-well plates and allowed to grow to 60-70% confluence. pKLO.1-puro plasmids encoding an MMP-1-specific short hairpin (sh)RNA (cat. no. TRCN0000372996) or a control scrambled shRNA (cat. no. SHC002) were purchased from Sigma-Aldrich (Merck KGaA). The pBasi-hU6 Pur DNA plasmid (Takara Bio, Inc.) was used to construct an HIF-1 α shRNA plasmid. The sequences of shRNA targeting MMP-1, HIF-1 α and control scrambled shRNA were designed as follows: MMP-1 (5'-CTT GAAGCTGCTTACGAATTT-3'), HIF-1 α (5'-CCACATTCA CGTATATGAT-3') and scrambled (5'-CAACAAGATGAA GAGCACCA-3'). The 58As9 cells were transfected with the plasmids (at a concentration of 2.5 μ g/2 ml of media) at 37°C for 48 h using Lipofectamine[®] 3000 (Thermo Fisher Scientific, Inc.) in accordance with the manufacturer's instructions. Cells stably expressing MMP-1-shRNA, HIF-1 α -shRNA and control shRNA (referred to as SC) were selected using

puromycin. Transfected cells were used in the experiment within 2 months.

Cell proliferation assay. Cell proliferation was assessed by growth curve analysis. For each cell line, 5.0×10^4 cells were incubated at 37°C for 24, 48 and 72 h. The cells were trypsinized and counted using a light microscope.

5-Aza-2-deoxycytidine (5-Aza-dC) and trichostatin A (TSA) treatments. The GC cell lines were treated with the demethylating agent 5-Aza-dC (Sigma-Aldrich; Merck KGaA) at 5 μ M for 72 h at 37°C, with drug replacement every 24 h. For the last 24 h, cells were also exposed to the histone deacetylase inhibitor TSA (Sigma-Aldrich; Merck KGaA) at 500 nM. Cells were harvested and used for RNA isolation.

Mouse studies. All methods were performed in accordance with the relevant guidelines and regulations. All animal protocols were approved by the Animal Care Committee of Saga University (approval no. A2020-015-0). A total of 20 of five-week-old female BALB/c nude mice were obtained from CLEA Japan, kept under specific-pathogen-free conditions and given sterile food and autoclaved water. The animals were maintained in an animal facility in a 12-h light/dark cycle in a temperature (20°C) and humidity (50%)-controlled environment. Food and water were freely available. Body weights were also measured twice per week.

Humane endpoints were reached when the xenograft tumor reached >10% of the animal body weight, the tumor diameter was >20 mm, tumors metastasized or grew such that it led to rapid body weight loss (>20%), or signs of immobility, a huddled posture, inability to eat, ruffled fur, self-mutilation, ulceration, infection or necrosis were observed. The mice that reached study endpoints were sacrificed by cervical dislocation.

Subcutaneous xenograft mouse models. The flanks of nude mice (as above; n=5) were injected subcutaneously with 3×10^6 58As9-SC or 58As9-MMP-1 knockdown cells. Tumor volume was calculated as follows: $T = \pi/4 \times a \times b$, where a (mm) is the shorter axis and b (mm) is the longer axis.

Peritoneal dissemination of xenografts. MMP-1 knockdown and SC cells (2×10^6) were suspended in 200 μ l of PBS and injected on day 0 into the abdominal cavity. A total of five mice per group were injected with each cell line. Mice that accumulated a large amount of ascites, became extremely debilitated, or lost a certain amount of weight were sacrificed and all mice were sacrificed on day 28. The total weights of the disseminated nodules in mice that were injected with MMP-1 knockdown and SC cells were measured. Body weight was also measured on days 3-24.

Patients. A total of 161 patients with advanced GC who consecutively underwent curative surgery at the Department of Surgery, Saga University Hospital (Saga, Japan), between June 2000 and December 2008 were enrolled in the present study. None of the patients presented with hepatic, peritoneal, or distant metastasis or tumor cells in the peritoneal fluid. Stage classification was performed in accordance with the

Table I. Characteristics of 161 patients and the tumors.

Characteristic	n (%)
Patients, n (%)	161 (100.0)
Age, years	
Median \pm SD (Range)	69 \pm 11.1 (26-88)
Sex, n (%)	
Female	54 (33.5)
Male	107 (66.5)
Surgery, n (%)	
Distal	69 (42.9)
Total	91 (56.5)
Proximal	1 (0.6)
Histology, n (%)	
Differentiated	66 (41.0)
Undifferentiated	95 (59.0)
Tumor depth, n (%)	
2	42 (26.1)
3	70 (43.5)
4a	43 (26.7)
4b	6 (3.7)
Lymph node metastasis, n (%)	
0	59 (36.6)
1	34 (21.1)
2	24 (14.9)
3a	16 (9.9)
3b	28 (17.4)
Lymphatic invasion, n (%)	
No	32 (19.9)
Yes	129 (80.1)
Vascular invasion, n (%)	
No	84 (52.2)
Yes	77 (47.8)
Stage, n (%)	
IB	25 (15.5)
IIA	36 (22.4)
IIB	23 (14.3)
IIIA	27 (16.8)
IIIB	25 (15.5)
IIIC	25 (15.5)
Adjuvant, n (%)	
No	98 (60.9)
Yes	63 (39.1)
Recurrence, n (%)	
No	106 (65.8)
Yes	55 (34.2)
Peritoneal dissemination	
Liver	19 (11.8)
Lymph node	18 (11.2)
Lung	12 (7.5)
Anastomosis	2 (1.2)
Pleural dissemination	2 (1.2)
Remnant Stomach	2 (1.2)
Spleen	1 (0.6)
Bone	1 (0.6)

Table I. Continued.

Characteristic	n (%)
MMP-1	
Low	121 (75.2)
High	40 (24.8)
MMP-1, matrix metalloproteinase-1.	

8th edition of the UICC TNM Classification (<https://www.uicc.org/resources/tnm>). The clinicopathological characteristics of the patients were recorded (Table I).

IHC analysis. For IHC, paraffin blocks (20x30 mm) were first sectioned onto slides at a thickness of 4 μ m. To remove the paraffin, slides were soaked in xylene and then rehydrated in a graded alcohol series. For antigen retrieval, the tissue sections were treated with Heat Processor Solution pH9 (Nichirei Bioscience) at 100°C for 40 min and then blocked with 5% skimmed milk at 20°C for 20 min. IHC was performed automatically using an Autostainer Plus (Dako; Agilent Technologies, Inc.). Antibodies against MMP-1 (dilution 1:200; cat. no. 52631; Abcam), Ki67 (dilution 1:2; cat. no. IR626, Dako; Agilent Technologies, Inc.) and the EnVision⁺ System (ready-to-use; cat. no. K5007; Dako; Agilent Technologies, Inc.) were used at room temperature as the primary and secondary antibodies, respectively. The slides were visualized using 3,3'-diaminobenzidine tetrahydrochloride and nuclei were counterstained with hematoxylin at room temperature for 2 min.

IHC analysis of MMP1 levels. The proportion of cells with positive MMP-1 cytoplasmic staining was assessed in the central region of the tumors and semi-quantitatively scored by a certified pathologist. The proportion of stained cells was evaluated in three fields of hotspot areas at high power (magnification, x200), scored from 0-100% and classified into the low or high expression group with 30% as the threshold between them.

IHC analysis of Ki67 levels. Immunostained tissue slides were digitized using a NanoZoomer 2.0HT digital slide scanner (Hamamatsu Photonics K.K.) and the resulting whole-slide digital images in NDPi files were visualized using NDP.view2 software (Hamamatsu Photonics K.K.). NDPi files were converted to JPEG files using NDP.view 2 software for imaging analysis. The rate of Ki67 positivity was automatically calculated by image analysis software (Tissue Studio[®] 4.0; Definiens AG), using five fields (magnification, x200) of hotspot areas for surgically resected specimens and three fields (magnification, x200) for mouse specimens selected by a certified pathologist.

Statistical analysis. All statistical analysis was performed using JMP Pro version 14 (SAS Institute, Inc.). Data are expressed as the mean \pm standard error. *In vitro* studies were performed in triplicate and repeated three times. Data were

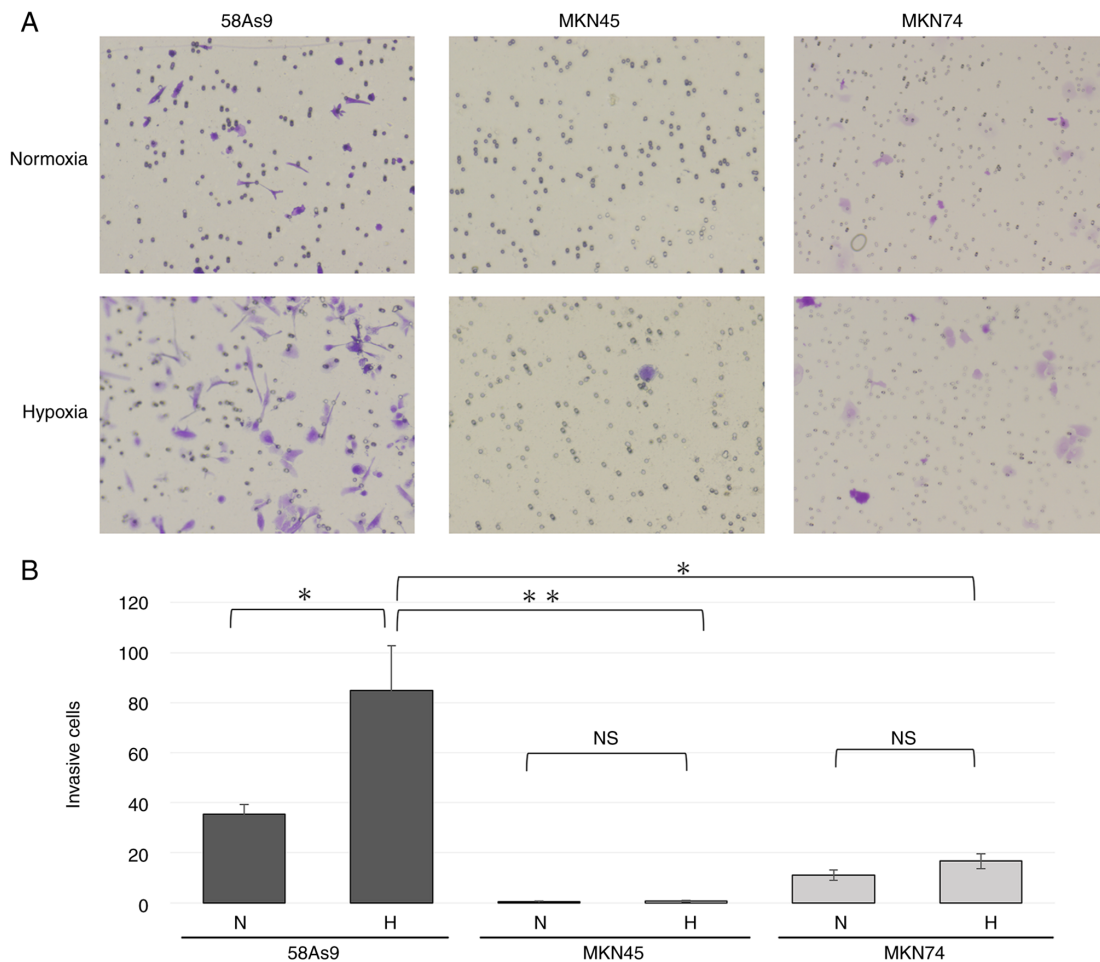


Figure 1. Analysis of invasion in GC cell lines under normoxia and hypoxia. (A) Transwell invasion assay of 58As9, MKN45 and MKN74 GC cells after incubation under normoxia or hypoxia for 24 h. Cells were stained with crystal violet (magnification, x20). (B) Quantification of invaded cells. Mean \pm standard error of the mean of n=3. *P<0.05, **P<0.01; NS, not significant. N, normoxia; H, hypoxia.

analyzed using Student's t-test when comparing two groups. Comparisons among multiple groups were analyzed using one-way ANOVA followed by Tukey's post hoc test. χ^2 analysis was used to analyze the correlation between MMP1 expression in GC and clinicopathological features and recurrences. A Cox proportional hazards model was used in the univariate and multivariate analyses of disease-free survival (DFS) and disease-specific survival (DSS). Kaplan-Meier curves of patients with high or low MMP-1 levels were plotted and log-rank tests were conducted. P<0.05 was considered to indicate a statistically significant difference.

Results

Invasiveness of GC cell lines. The invasiveness of 58As9, MKN45 and MKN74 GC cells was evaluated by a Transwell invasion assay and compared. The number of invaded 58As9 cells was significantly higher compared with the other cell lines under normoxia. In addition, the number of 58As9 cells was significantly elevated under hypoxia compared with that under normoxia (Fig. 1A and B). These results indicated that hypoxia increased the invasiveness of the GC cell line 58As9, whereas the other two cell lines exhibited limited invasiveness under both normoxia and hypoxia.

MMP-1 expression in GC cell lines. To clarify the mechanism of hypoxia-induced invasion in 58As9 cells, the expression of the invasion-related enzyme MMP-1 was evaluated in 58As9, MKN45 and MKN75 cells by RT-qPCR analysis (Fig. 2A). MMP-1 mRNA expression was detected only in 58As9 cells under normoxia and the level was significantly elevated under hypoxia (Fig. 2A). The protein expression of MMP1 and HIF-1 α was next investigated by WB analysis (Fig. 2B). HIF-1 α expression was induced in all three cell lines under hypoxia for 12, 24 and 48 h, compared with those under normoxia. By contrast, MMP1 expression was induced in hypoxic 58As9 cells for 24 and 48 h; however, the expression was undetectable in MKN45 or MKN74 cells under both normoxia and hypoxia.

Regulation of MMP-1 expression in 58As9 cells. To investigate the regulation of hypoxia-induced MMP-1 expression in 58As9 GC cells, both HIF-1 α knockdown and MMP-1 knockdown cells were analyzed (Fig. 3A). The relative expression of MMP-1 mRNA was significantly decreased in HIF-1 α knockdown and MMP-1 knockdown cells under hypoxia compared with that in SC cells. WB analysis revealed that the hypoxia-induced expression of HIF-1 α and MMP-1 was decreased in HIF-1 α knockdown cells compared with that in control SC cells.

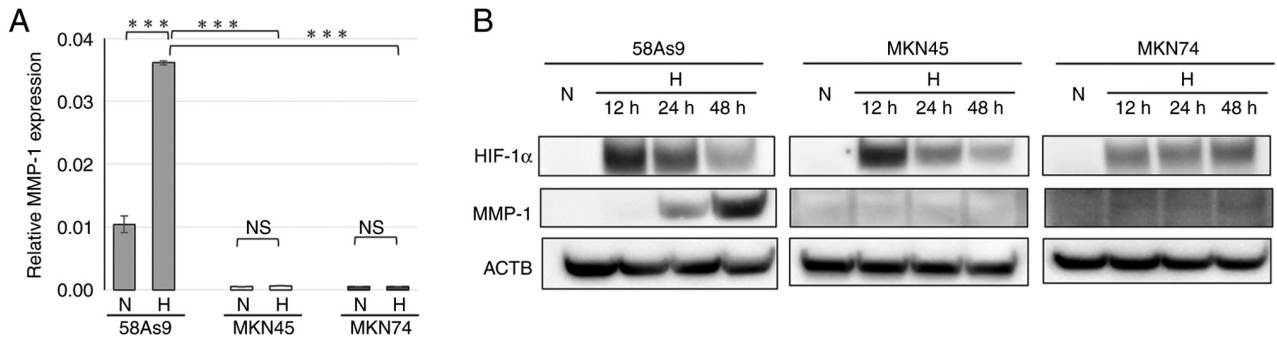


Figure 2. Expression of MMP-1 in three GC cell lines. (A) Reverse transcription-quantitative PCR analysis of MMP-1 expression in 58As9, MKN45 and MKN74 cells following incubation under normoxia or hypoxia for 24 h. Mean \pm standard error of the mean is plotted in the graph. *** $P < 0.001$; NS, not significant. (B) Western blot analysis of HIF-1 α (upper panel) and MMP-1 (middle panel) in GC cells after incubation under normoxia for 24 h or hypoxia for 12, 24 and 48 h. MMP-1, matrix metalloproteinase-1; GC, gastric cancer; HIF-1 α , hypoxia-inducible factor-1 α ; N, normoxia; H, hypoxia; ACTB, β -actin.

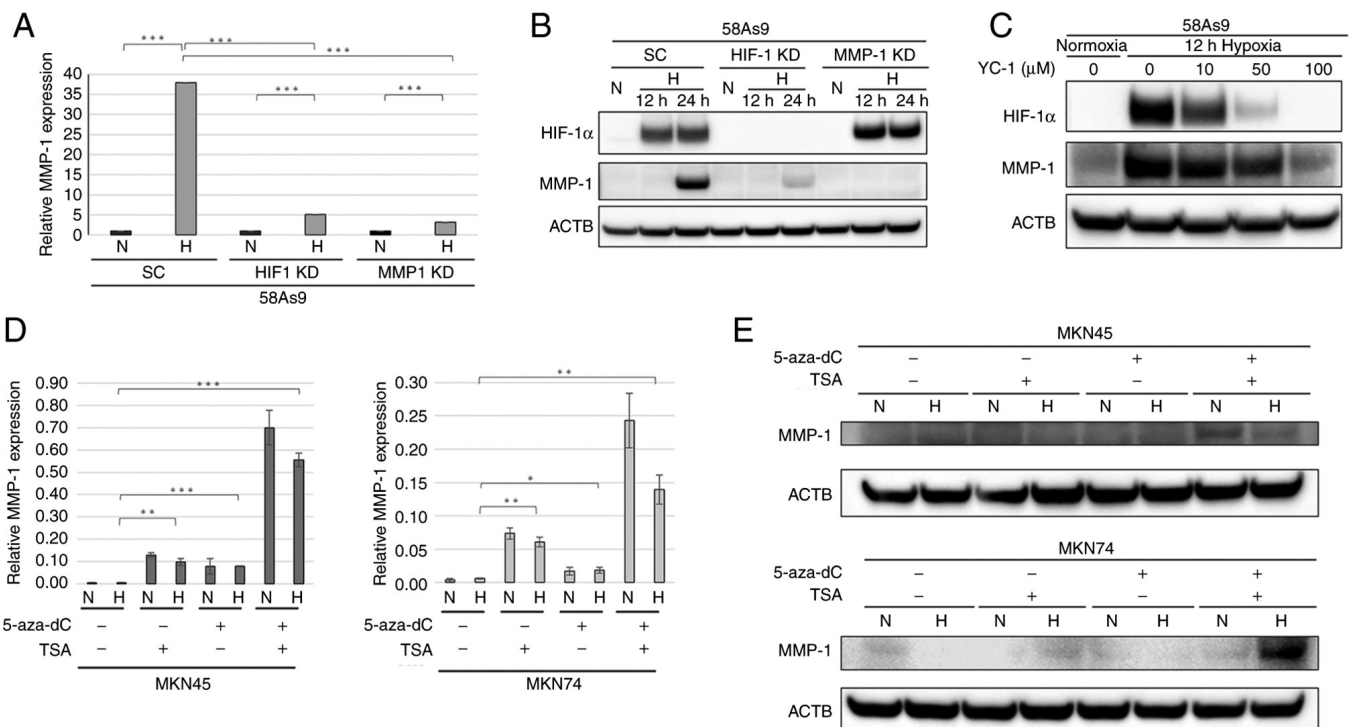


Figure 3. Assessment of MMP-1 expression in HIF-1 α knockdown and MMP-1 knockdown cells. (A) RT-qPCR of MMP-1 in MMP-1 knockdown, HIF-1 α knockdown and SC cells. (B) WB analysis of MMP-1 and HIF-1 α in MMP-1 knockdown and HIF-1 α knockdown cells. SC cells were used as a control. (C) WB analysis of HIF-1 α and MMP-1 expression in 58As9 cells treated with YC-1 (0-100 μ M) for 12 h under normoxia and hypoxia. (D) RT-qPCR of MMP-1 in MKN45 and MKN74 cells treated with 5-Aza-dc (5 μ M) for 72 h and/or TSA (500 nM) for 24 h. Mean \pm standard error of the mean is plotted in the graph. * $P < 0.05$, ** $P < 0.01$, *** $P < 0.001$. (E) WB analysis of MMP-1 expression in MKN45 and MKN74 cells treated with 5-Aza-dc and/or TSA under normoxia and hypoxia. MMP-1, matrix metalloproteinase-1; RT-qPCR, reverse transcription-quantitative PCR; HIF-1 α knockdown, hypoxia-inducible factor-1 α knockdown; WB, western blotting; SC, scramble; N, normoxia; H, hypoxia; 5-aza-dC, 5-Aza-2-deoxycytidine; TSA, Trichostatin A; ACTB, β -actin.

Furthermore, MMP-1 expression was completely abolished in MMP-1 knockdown cells, whereas hypoxia-induced HIF-1 α expression was preserved in MMP-1 knockdown cells (Fig. 3B). Whether the HIF-1 α inhibitor YC-1 influences hypoxia-induced MMP-1 expression was next analyzed. As shown in Fig. 3C, the expression of both HIF-1 α and MMP-1 was dose-dependently decreased in YC-1-treated 58As9 cells under hypoxia. Taken together, these results indicated that hypoxia-induced MMP-1 expression was directly regulated by HIF-1 α in 58As9 cells. To further investigate the mechanisms underlying deficient MMP-1 expression in MKN45 and MKN74 cells, the present study focused on epigenetic gene

silencing. Thus, whether MMP-1 expression was restored by treatment with the demethylating agent 5-aza-dC and/or the histone deacetylase inhibitor TSA in these cells was analyzed (Fig. 3D). In the two cell lines, MMP1 mRNA expression was significantly increased by either of these treatments under normoxia and hypoxia compared with that in the absence of treatment. In addition, combined treatment with 5-aza-dC and TSA markedly increased MMP-1 expression compared with that upon 5-aza-dC or TSA treatment alone (Fig. 3D). However, the hypoxic induction of MMP-1 expression was not observed in a series of experiments in the present study. In WB analysis, combined 5-aza-dC and TSA treatments increased

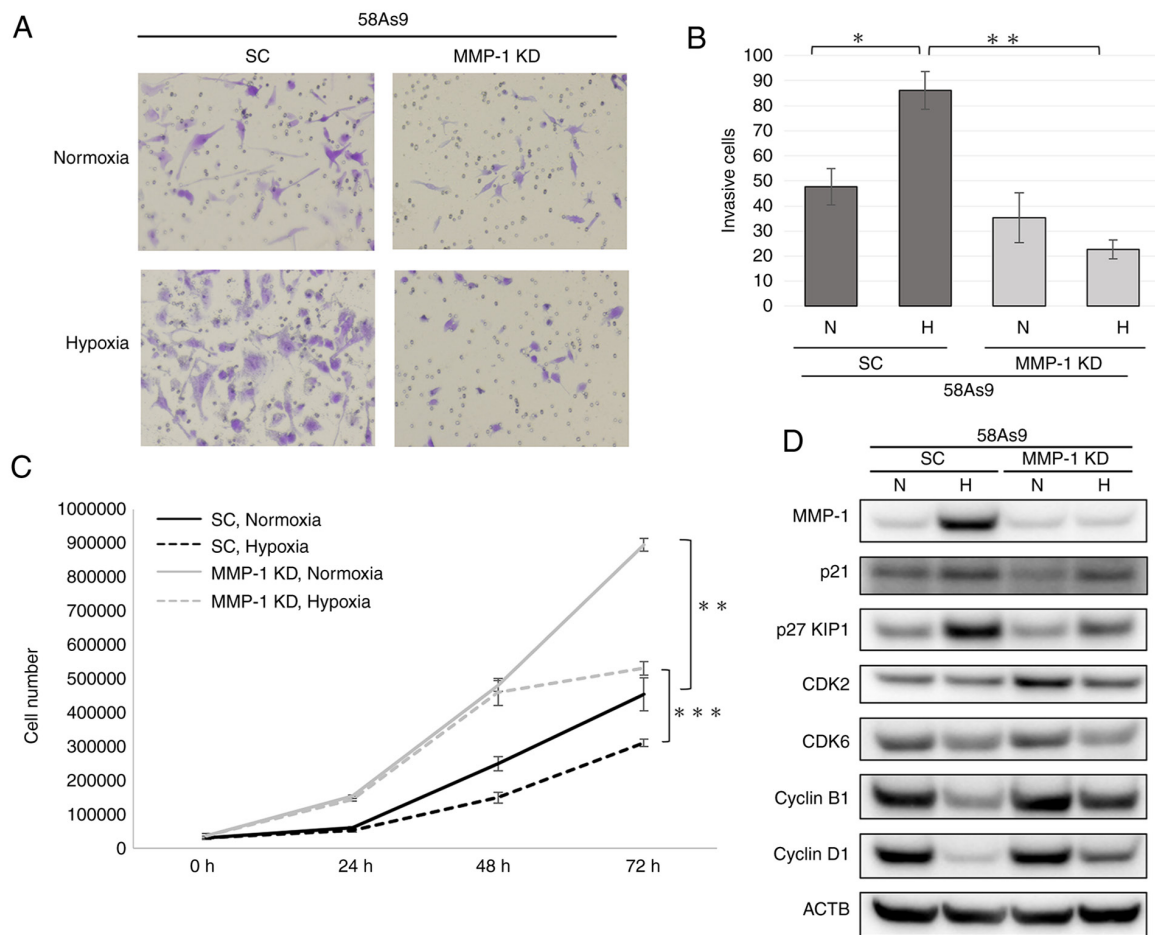


Figure 4. Assessment of the invasive and proliferative abilities of MMP-1 knockdown cells. (A) Transwell invasion assay of SC and MMP-1 knockdown cells after incubation under normoxia or hypoxia for 24 h (magnification, x20). (B) Quantification of invaded cells. (C) Cell proliferation curve of SC and MMP-1 knockdown cells. For each cell line, 5.0×10^4 cells were incubated under normoxia or hypoxia for 24, 48 and 72 h. Mean \pm standard error of the mean was plotted in the graph. * $P < 0.05$, ** $P < 0.01$, *** $P < 0.001$. (D) Western blot analysis of cell cycle-related proteins including p21, p27 KIP1, CDK2, CDK6, cyclin B1 and cyclin D1 in MMP-1 knockdown and SC cells. MMP-1 expression was confirmed in SC, but not in MMP-1 knockdown cells. MMP-1, matrix metalloproteinase-1; SC, scramble; KD, knockdown; CDK, cyclin-dependent kinase; N, normoxia; H, hypoxia; 5-aza-dC, 5-Aza-2-deoxycytidine; TSA, Trichostatin A; ACTB, β -actin.

MMP-1 expression in MKN74 and MKN45 cells (Fig. 3E). This demonstrated that an epigenetic mechanism is involved in the deficient MMP-1 expression in MKN45 and MKN74 GC cells.

Effects of MMP-1 knockdown on invasion and proliferation of 58As9 cells. The effect of MMP-1 knockdown on cancer invasion and proliferation was evaluated using MMP-1 knockdown and SC cells (Fig. 4A). Hypoxia appeared to increase the invasion of 58As9-SC cells (Fig. 4A). By contrast, the invasion of MMP-1 knockdown cells was similar under normoxia and hypoxia (Fig. 4A). Quantitatively, the number of invaded SC cells was significantly elevated under hypoxia compared with that under normoxia (Fig. 4B). However, the numbers of invaded MMP-1 knockdown cells were similar under hypoxia and normoxia (Fig. 4B). Consequently, the number of invaded SC cells was significantly higher than that of MMP-1 knockdown cells under hypoxia (Fig. 4B).

To evaluate the proliferative ability of SC and MMP-1 knockdown cells, cell numbers were measured under normoxia and hypoxia at 24, 48 and 72 h (Fig. 4C). At 72 h, the number of MMP-1 knockdown cells was significantly higher than that of SC cells under both normoxia and hypoxia (Fig. 4C).

To further investigate the difference of cell proliferation between SC and MMP-1 knockdown cells, the expression of cell cycle-related genes including p21, p27 KIP1, cyclin-dependent kinase (CDK)2, CDK6, cyclin B1 and cyclin D1 was assessed by WB (Fig. 4D). Under normoxia, p21 expression was reduced in MMP-1 knockdown cells, compared with that in SC cells. By contrast, CDK2 expression was higher in MMP-1 knockdown compared with SC cells. Under hypoxia, p27 KIP1 expression was attenuated in MMP-1 knockdown compared with that in SC cells. However, the expression of cyclin B1 and cyclin D1 was elevated in MMP-1 knockdown cells compared with that in SC cells. These results indicated that the acceleration of cell growth by MMP-1 knockdown may be due to the attenuation of p21 and increased CDK2 expression under normoxia. Furthermore, reduced p27 KIP1 expression and increased cyclin B1 and cyclin D1 expression may contribute to the higher growth of MMP-1 knockdown cells than that of SC cells under hypoxia.

Effect of MMP-1 knockdown on the growth of xenograft tumors in mice. The *in vivo* effect of MMP-1 knockdown on tumor growth in mice was next evaluated. MMP-1 knockdown and 58As9 SC cells were subcutaneously injected into nude

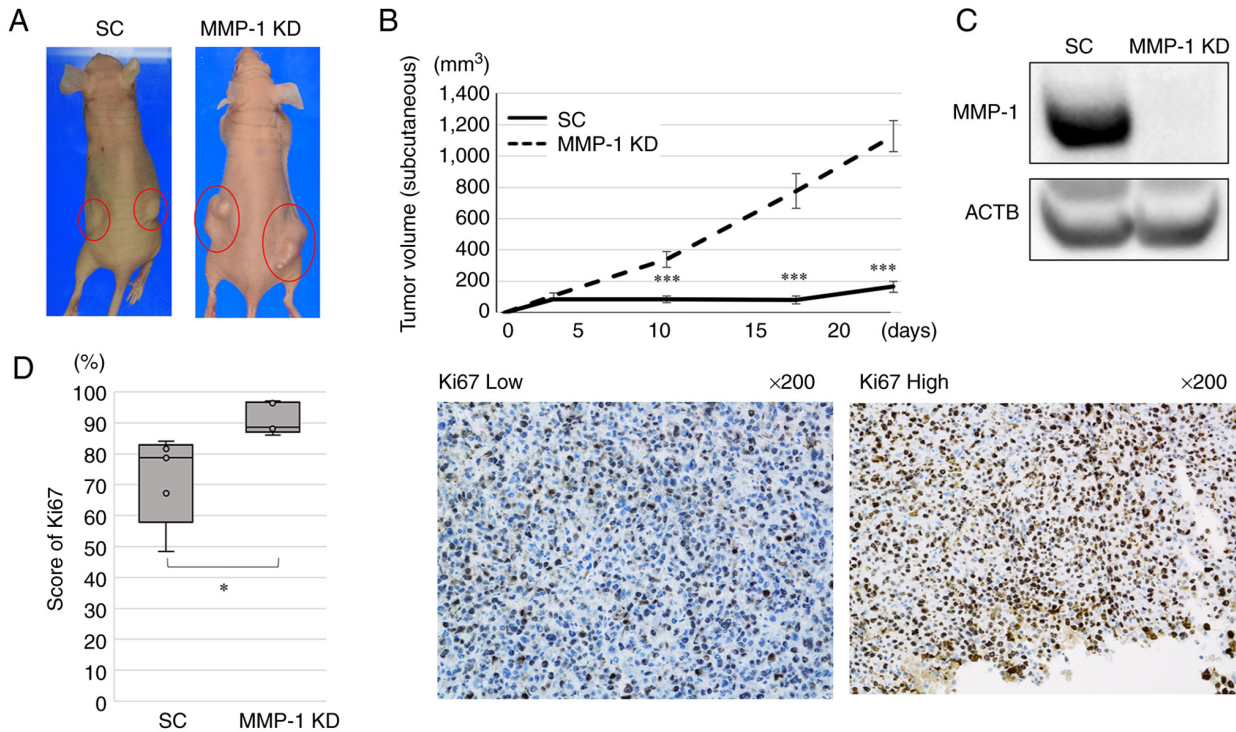


Figure 5. Effect of MMP-1 knockdown on tumor growth in mice. (A) Macroscopic appearance of the nude mice that underwent subcutaneous injection of MMP-1 knockdown and SC cells. Tumor area is surrounded by a red circle. (B) Volume of MMP-1 knockdown and SC xenograft tumors on days 5-20 was plotted in the graph. Mean \pm standard error of the mean was plotted in the graph. *** $P < 0.001$. (C) Western blot analysis of MMP-1 expression in the xenograft tumors. (D) Comparison of Ki67 score in subcutaneous tumor between SC and MMP-1 knockdown cells. Representative images with low and high Ki67. Mean \pm standard error of the mean. * $P < 0.05$. MMP-1, matrix metalloproteinase-1; SC, scramble; KD, knockdown; ACTB, β -actin.

mice and the sizes of subcutaneous tumors were measured. Then, 24 days after subcutaneous injection, the xenograft tumors from MMP-1 knockdown cells appeared larger than those from SC cells (Fig. 5A). The maximum diameter of the tumor in all mice was 17 mm and the maximum volume was 1,601 mm³. The mean tumor volumes measured on days 10, 18 and 24 after the subcutaneous injection were significantly higher in MMP-1 knockdown compared with SC tumors (Fig. 5B). WB analysis confirmed the deficient MMP-1 expression in MMP-1 knockdown cells (Fig. 5C).

The number of Ki67-positive cells in the xenograft tumors were estimated by IHC analysis. The mean score of Ki67 was significantly higher in MMP-1 knockdown tumors (mean: 91.2%, range: 88.0-97.1%) compared with SC tumors (mean: 72.0%, range: 48.4-84.1%; $P = 0.025$; Fig. 5D).

Effect of MMP-1 knockdown on development of peritoneal dissemination in mice. MMP-1 knockdown and SC cells were intraperitoneally injected into mice and the ability to form peritoneal dissemination was evaluated. All mice intraperitoneally injected with MMP-1 knockdown developed ascites by day 25, whereas those with SC cells did not (Fig. 6A). Disseminated nodules in the peritoneal cavity were formed in all five mice (100%) injected with MMP-1 knockdown, while they were observed in three of the five mice (60%) injected with SC (Fig. 6B). The total weight of the disseminated nodules was significantly greater in MMP-1 knockdown (1.024 g) compared with SC (0.2618 g) ($P < 0.001$) (Fig. 6C). Mean body weight of MMP-1 knockdown mice gradually increased with time due to the ascites (Fig. 6D). On day 21, mean body weight

was significantly greater in MMP-knockdown compared with SC mice (Fig. 6D).

IHC analysis of MMP-1 in GC tissues. MMP-1 expression levels were evaluated by IHC in 161 advanced GC tissues. High MMP-1 expression was identified in 40 (24.8%) of the 161 patients, whereas low MMP-1 expression was observed in the rest. Fig. 7 shows the IHC results of MMP-1 expression. A representative tissue sample with low MMP-1 expression is shown in Fig. 7A. By contrast, MMP-1 expression was observed in the cytoplasm of GC cells in cases with high MMP-1 expression (Fig. 7B). Furthermore, MMP-1-positive cells were mainly localized at the surface of cancer tissues (Fig. 7C). In addition, MMP-1 was not stained at the stroma in almost GC tissues, although it was slightly stained in some cases (Fig. 7B and C). We further evaluated proliferation in 161 GC tissues by Ki67 IHC analysis. The mean Ki67-positive rate was significantly higher in the Low MMP-1 group (mean: 30.7%, range: 4.3-61.9%) compared with the High group (mean: 20.7%, range: 2.7-52.5%; $P < 0.001$; Fig. 7D).

Relationship between MMP-1 expression and clinicopathological factors. The associations of the MMP-1 expression level with clinicopathological factors were statistically analyzed (Table II). MMP-1 expression was significantly associated with age, histology and cancer recurrence (Table II). The Low MMP-1 group had a higher proportion of patients >70 years of age compared with the High MMP-1 group ($P = 0.015$). Regarding cancer histology, the proportion of undifferentiated types was significantly higher in the Low MMP-1 group (78/121, 64.5%) compared with the High MMP-1 group (17/40,

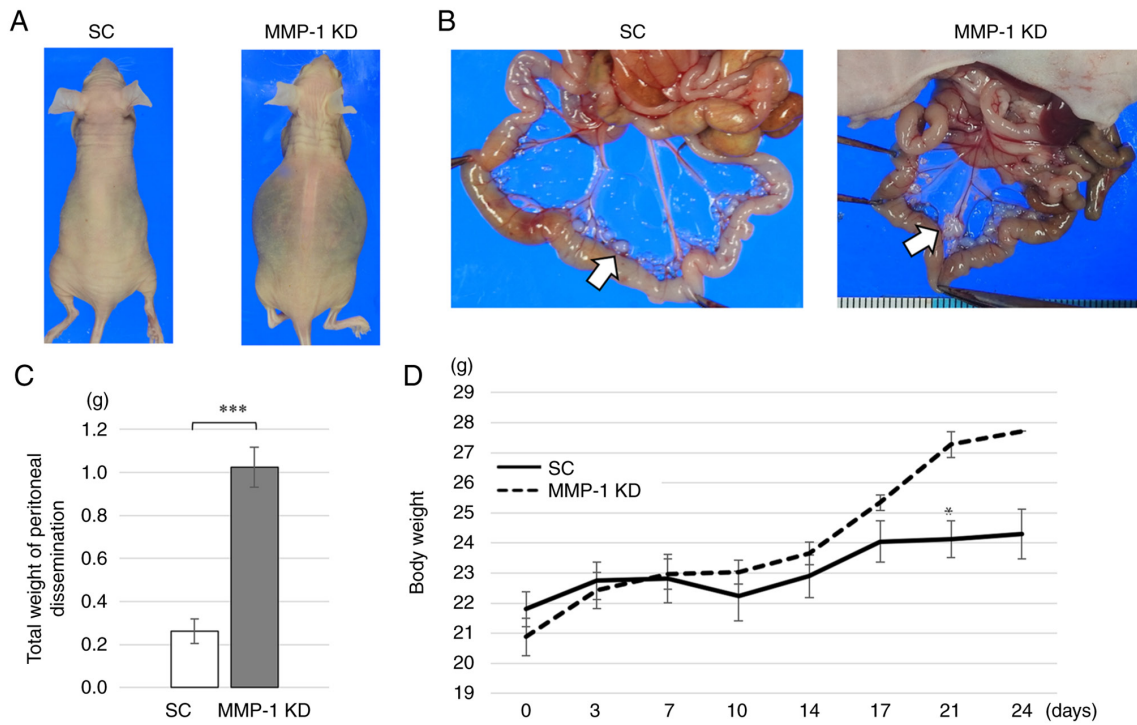


Figure 6. Effect of MMP-1 knockdown on peritoneal dissemination in mice. (A) Macroscopic appearance of mice in which MMP-1 knockdown or SC cells were intraperitoneally injected. (B) Macroscopic appearance of the peritoneal dissemination in mice. Disseminated nodules are indicated by arrows (magnification, x1). (C) Total weight of disseminated tumors in SC and MMP-1 knockdown mice. (D) Change of body weight in SC and MMP-1 knockdown mice. Mean \pm standard error of the mean. * $P < 0.05$; *** $P < 0.001$. MMP-1, matrix metalloproteinase-1; SC, scramble; KD, knockdown.

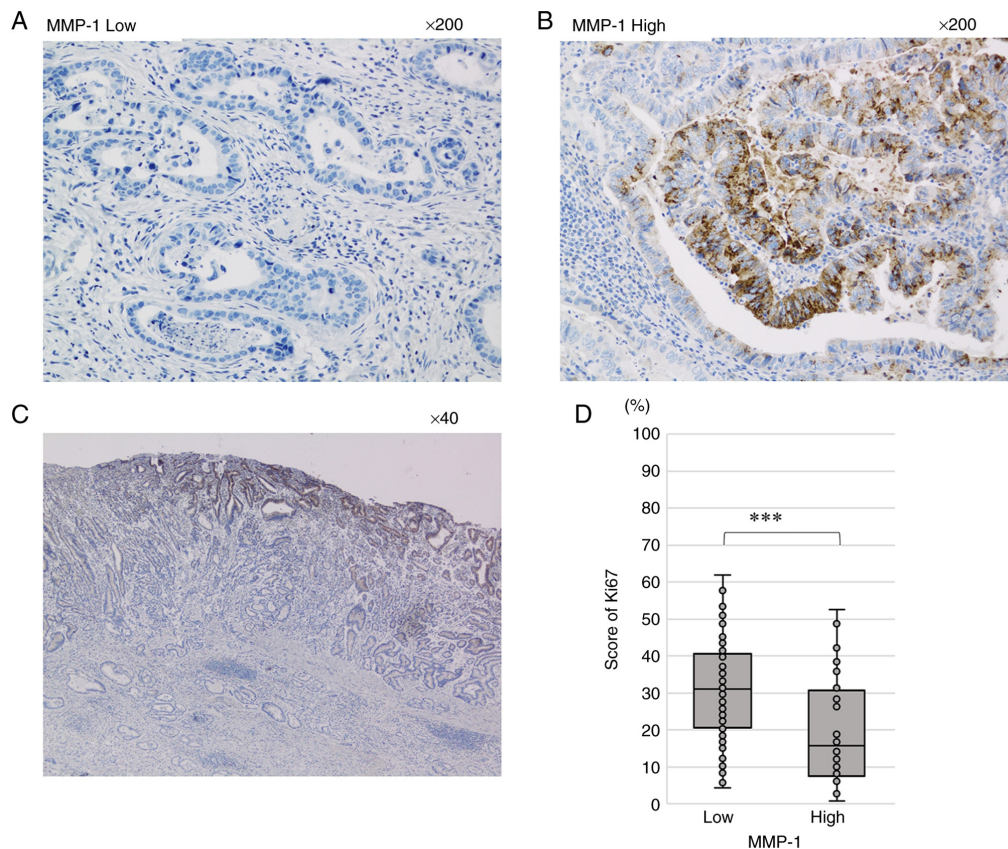


Figure 7. Immunohistochemical analysis of MMP-1 and Ki67. (A) Tissue sample classified as having low MMP-1 expression (magnification, x200). MMP-1 staining was negative. (B) Tissue sample classified as having high MMP-1 expression (x200). Positivity for MMP-1 staining was observed in the cytoplasm of GC cells. (C) Image of the same case as shown in panel B (magnification, x40). GC cells with positive staining were mainly localized at the tumor surface. (D) Comparison of Ki67 scores between groups with high and low MMP-1 expression. Mean \pm standard error of the mean is plotted in the graph. *** $P < 0.001$. MMP-1, matrix metalloproteinase-1; GC, gastric cancer.

Table II. Correlation between MMP-1 expression and clinicopathological features.

	High MMP-1 (n=40)		Low MMP-1 (n=121)		P value
	n	%	n	%	
Age, years (mean±SD)	66.1±9.57		69.4±11.59		0.015
<70	26	33.3	52	66.7	0.581
>70	14	16.9	69	83.1	
Sex					0.581
Male	28	26.2	79	73.8	0.015
Female	12	22.2	42	77.8	
Histology					0.015
Differentiated	23	34.8	43	65.2	0.146
Undifferentiated	17	17.9	78	82.1	
Tumor depth					0.146
2	14	33.3	28	66.7	0.613
3/4	26	21.8	93	78.2	
Lymph node metastasis					0.613
No	16	27.1	43	72.9	0.651
Yes	24	23.5	78	76.5	
Lymphatic invasion					0.651
No	9	27.3	24	72.7	0.714
Yes	31	24.2	97	75.8	
Vascular invasion					0.714
No	20	23.8	64	76.2	0.129
Yes	20	26.3	56	73.7	
Stage					0.129
I	25	29.8	59	70.2	0.383
II/III	15	19.5	62	80.5	
Adjuvant therapy					0.383
No	22	22.4	76	77.6	0.009
Yes	18	28.6	45	71.4	
Recurrence					0.009
No	33	30.8	74	69.2	0.096
Yes	7	13.0	47	87.0	
Peritoneal dissemination					0.096
No	38	26.4	106	73.6	
Yes	2	11.8	15	88.2	

MMP-1, matrix metalloproteinase-1.

42.5%) (P=0.015). Recurrent cancer was more frequently observed in the Low MMP-1 group (47/121, 38.8%) compared with the High MMP-1 group (7/40, 17.5%) (P=0.009). In addition, 17 cases of peritoneal dissemination were observed among 54 cases of recurrent cancer. Peritoneal dissemination demonstrated a tendency to be more common in the Low MMP-1 group (12.4%) compared with the High group (5.0%) (P=0.096).

Relationship between MMP-1 expression and patient survival. The association between patient survival and MMP-1

expression was analyzed in the 161 patients with advanced GC (Fig. 8). Kaplan-Meier curve analysis and log-rank test demonstrated that the DFS in GC patients with low MMP-1 expression (n=121) was significantly shorter compared with those with high expression (P=0.005) (Fig. 8A). The DSS was also shorter in patients with low MMP-1 expression (n=121) compared with those with high expression (n=40) (P=0.022) (Fig. 8B).

Univariate analysis of 161 patients demonstrated that tumor depth (T), lymph node metastasis (N), lymphatic invasion (Ly), stage and MMP-1 expression were significantly associated with

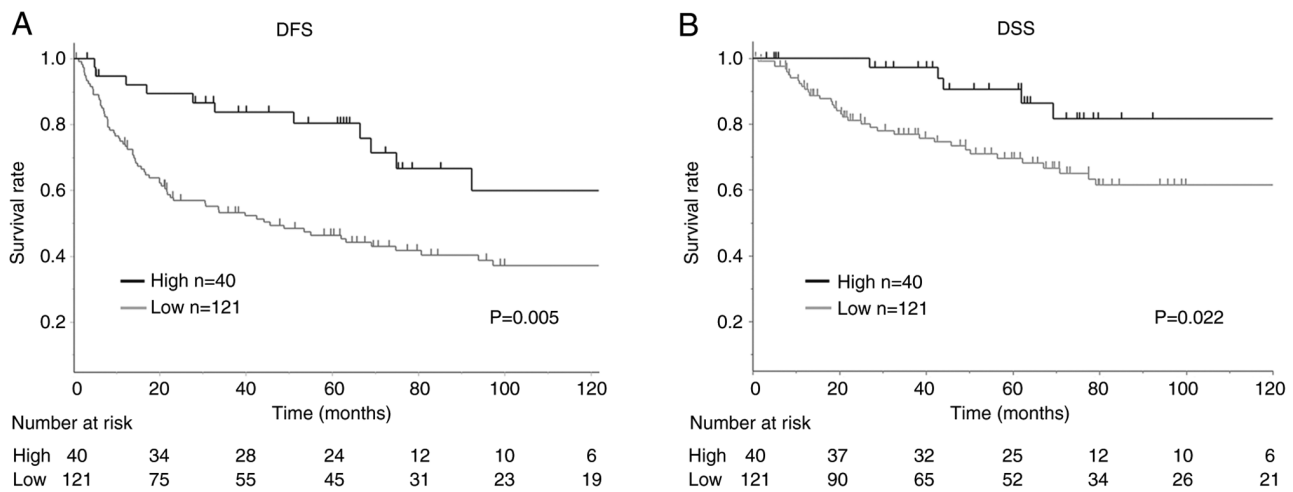


Figure 8. Survival curves of 161 GC patients with high and low MMP-1 expression. (A) Kaplan-Meier estimates of DFS. (B) Kaplan-Meier estimates of DSS. GC, gastric cancer; MMP-1, matrix metalloproteinase-1; DFS, disease-free survival; DSS, disease-specific survival.

DFS (Table III). Multivariate analysis further confirmed that N and MMP1 expression were factors independently predictive of DFS (Table III). Another univariate analysis demonstrated that T, N, Ly, vascular invasion (V), stage, adjuvant chemotherapy and MMP-1 expression were significantly associated with DSS (Table III). The multivariate analysis revealed that N, V and MMP1 expression were factors independently predictive of DSS (DFS: HR=2.111; 95% CI: 1.222-3.920; P=0.005; DSS: HR=2.899; 95% CI: 1.234-8.499; P=0.012; Table III).

Discussion

The majority of solid tumors maintain growth under hypoxic environments. Tumor hypoxia generally promotes the malignant behavior of cancer cells, such as invasion and metastasis (3). The present study analyzed three GC cell lines: 58As9, MKN45 and MKN74. First, it demonstrated the increased invasiveness of 58As9 cells under hypoxia, whereas the other two cell lines-MKN45 and MKN74-exhibited limited invasiveness. Next, it was attempted to identify an HIF-1 α target gene that is specifically expressed in 58As9 cells and required for their enhanced invasion under hypoxia. RT-qPCR analysis of invasion-related genes, such as RHOA, ROCK1, S100A4, UPAR, MMP-7, MMP-14, AMFR, LOXL2, C-MET and MMP-1, was performed using three GC cell lines (48-56). The results demonstrated that hypoxia-induced elevation of MMP-1 mRNA occurred in 58As9 cells, but not in the other two cell lines. By contrast, the other nine genes did not show the hypoxia-induced elevation of the corresponding mRNA specifically in 58As9 cells (data not shown). Therefore, the present study focused on MMP-1 and investigated the biological roles of GC cells under hypoxia. To clarify whether the hypoxia-induced expression of MMP-1 was dependent on HIF-1 α , HIF-1 α knockdown cells were generated. The results revealed that the silencing of HIF-1 α expression in HIF-1 α knockdown cells markedly attenuated MMP-1 expression. Furthermore, hypoxia-induced MMP-1 expression was suppressed by drug treatment with the HIF-1 α inhibitor YC-1 in parental 58As9 cells. These results clearly demonstrated that MMP-1 expression was directly upregulated by HIF-1 α in

hypoxic 58As9 cells. In addition, combination treatment with 5-aza-dC and TSA significantly increased MMP-1 expression in MMP-1-deficient MKN45 and MKN74 cells, which suggested that epigenetic mechanisms, including chromatin supraorganization, may play an important role in silencing MMP-1 expression (57,58). Previously, the upregulation of MMP-1 by HIF-1 α has been reported in metastatic bladder cancer cells (59). Epigenetic regulation of MMP-1 expression is also reported in a previous study, in which 5-aza-dC plus TSA treatments increases MMP-1 mRNA expression in a human fibrosarcoma cell line (58). The present study demonstrated that both HIF-1 α -dependent and epigenomic mechanisms are involved in regulating MMP-1 expression in GC cell lines.

MMP-1 knockdown 58As9 cells were generated and the effect of MMP-1 knockdown on cell invasion and proliferation investigated. Hypoxia failed to enhance the invasiveness of MMP-1 knockdown cells, indicating that MMP-1 expression was essential for hypoxia-enhanced invasion in 58As9 cells. MMP-1 is a proteolytic enzyme that degrades type I and III collagens, which are the main components of the GC stroma (60,61). These reports support the finding of the present study that MMP-1 knockdown decreased the *in vitro* invasion of MMP-1-expressing 58As9 cells. By contrast, *in vitro* cell proliferation was increased in MMP-1 knockdown cells under both normoxia and hypoxia compared with that in control SC cells. It was further elucidated that the promotion of cell proliferation by MMP-1 knockdown was derived from elevated expression of the cell cycle activators cyclin D1 and cyclin B1 and attenuated expression of the cell cycle repressors p21 and p27KIP1 (62-65). In nude mice, MMP-1 knockdown xenograft tumors also exhibited accelerated growth compared with SC tumors. The mean Ki67 score was higher in MMP-1 knockdown compared with SC tumors. Taken together, these results constituted novel evidence that MMP-1 acted as a suppressor of cell proliferation by altering the expression of cell cycle-related proteins in 58As9 GC cells.

Among cancer recurrences occurring in GC patients, peritoneal dissemination is the most common type (66). The present study thus explored the effect of MMP-1 knockdown on the development of peritoneal dissemination. The results

Table III. Univariate and multivariate analysis for disease free survival and disease specific survival in 161 patients.

A. Disease free survival						
Variable	Univariate			Multivariate		
	HR	95% C.I.	P-value	HR	95% C.I.	P-value
Age, years <70 / >70	0.745	(0.484-1.142)	0.177			
Sex Male/Female	1.481	(0.940-2.414)	0.091			
Histology Differentiated/Undifferentiated	1.057	(0.681-1.620)	0.801			
Tumor depth 2/3-4	0.524	(0.289-0.886)	0.015	0.708	(0.379-1.244)	0.352
Lymph node metastasis -/+	0.428	(0.263-0.676)	<0.001	0.456	(0.253-0.796)	0.004
Lymphatic invasion -/+	0.569	(0.308-0.976)	0.040	0.996	(0.496-1.903)	0.989
Vascular invasion -/+	0.691	(0.454-1.050)	0.084	0.720	(0.465-1.112)	0.108
Stage I-II/III	0.392	(0.251-0.602)	<0.001			
Adjuvant -/+	0.675	(0.445-1.029)	0.067	1.055	(0.646-1.710)	0.760
MMP1 -/+	2.084	(1.215-3.853)	0.007	2.111	(1.222-3.920)	0.005
B. Disease specific survival						
Variable	Univariate			Multivariate		
	HR	95% C.I.	P-value	HR	95% C.I.	P-value
Age, years <70 / >70	0.915	(0.491-1.698)	0.778			
Gender Male/Female	1.146	(0.605-2.287)	0.684			
Histology Differentiated/Undifferentiated	1.135	(0.598-2.105)	0.693			
Tumor depth 2/3-4	0.203	(0.049-0.560)	<0.001	0.322	(0.076-0.934)	0.036
Lymph node metastasis -/+	0.068	(0.011-0.223)	<0.001	0.072	(0.011-0.271)	<0.001
Lymphatic invasion -/+	0.256	(0.062-0.707)	0.006	1.326	(0.286-4.423)	0.686
Vascular invasion -/+	0.445	(0.227-0.838)	0.012	0.485	(0.239-0.939)	0.032
Stage I-II/III	0.152	(0.061-0.323)	<0.001			
Adjuvant -/+	0.478	(0.254-0.889)	0.019	1.108	(0.564-2.124)	0.760
MMP1 -/+	2.84	(1.221-8.272)	0.013	2.899	(1.234-8.499)	0.012

HR, hazard ratio; C.I., confidence interval; MMP-1, matrix metalloproteinase-1.

demonstrated that MMP-1 knockdown accelerated the formation of peritoneal dissemination in mice, compared with that for SC. The present study first demonstrated a suppressive role of MMP-1 in cell proliferation *in vitro*, tumor growth and development of peritoneal dissemination in mice, although MMP-1 served a critical role in hypoxia-induced invasion in 58As9 GC cell line *in vitro*. Peritoneal dissemination is hypothesized to develop through a direct seeding mechanism, which is composed of several steps including cancer invasion, attachment and proliferation distant peritoneum (67). The loss of MMP-1 expression in MMP-1 knockdown cells may increase adhesion and proliferation on the peritoneal peritoneum, while the loss may attenuate invasiveness.

On the basis of these findings in GC cell lines, the relationship between the IHC expression of MMP-1 and clinical outcomes of GC patients was investigated. Regarding clinicopathological factors, MMP-1 expression was significantly associated with age, histology and cancer recurrence. Studies using cancer tissues have reported that T, V and Ly are important parameters for cancer invasion (68). However, MMP-1 expression was not significantly associated with these invasion parameters in 161 GC tissues. One possible explanation of this is that the positive immunostaining for MMP-1 was mainly observed at the tumor surface rather than deeper areas, including the invasive tumor front. Therefore, MMP-1 expression may not be responsible for tumor invasion and the expression was not significantly associated with the invasion-related clinicopathological parameters. In addition, MMP-1 expression did not show a significant correlation with HIF-1 α expression (data not shown), which was previously analyzed using the same 161 GC tissues (69). One possible reason for this result is that, in GC tissues, MMP-1 expression is regulated not only by HIF-1 α , but also by an epigenetic mechanism. Methylation analysis of the MMP-1 gene promoter may be necessary to explain this finding. By contrast, the mean Ki67 score in the 161 GC tissues was higher in the Low MMP-1 group compared with the High group ($P < 0.001$). This may be consistent with the findings in the mouse xenograft model. In addition, patients with low MMP-1 expression exhibited significantly higher recurrence rates, indicating that GC with low MMP-1 expression has higher malignant potential than that with high expression. Among the cancer recurrences, the occurrence of peritoneal dissemination was more frequently observed in the Low MMP-1 group compared with the High group, although this did not reach statistical significance. This result may support the findings in nude mice. It may be necessary to analyze more GC patients in order to clarify the significance of this relationship. The present study analyzed the association between MMP-1 expression and patient survival. DFS and DSS were significantly shorter in the Low MMP-1 expression group compared with the High group. Multivariate analysis demonstrated that MMP-1 expression was an independent determinant of both DFS and DSS. IHC studies using cancer tissues previously identified a significant relationship between MMP-1 expression and patient outcome (34-45). In the majority of these studies, a significant association between high MMP-1 expression and poor patient prognosis was reported in esophageal, gallbladder and hepatocellular carcinoma (35,36,39). By contrast, another study reported that high MMP-1 expression is significantly

associated with an improved prognosis in prostate cancer (38), which appears to support the findings of the present study. In addition, Kosaka *et al* (70) reported that high level of MMP-1 mRNA expression in GC patients demonstrates a significant association with clinical stage and distant metastasis, although they analyzed expression of MMP-1 mRNA in bone marrow and peripheral blood, not in primary GC tissues. This shows that there is still controversy about the effect of MMP-1 expression on survival of patient with cancers.

In conclusion, the present study reported that MMP-1 expression was regulated in a distinct process by HIF-1 α -dependent and epigenomic mechanisms in GC cells. MMP-1 expression increased hypoxia-induced cancer invasion but inhibited the proliferation of 58As9 GC cells. Furthermore, MMP-1 expression acted as a repressor of xenograft tumor growth and the development of peritoneal dissemination in nude mice. In the IHC study of GC tissues, MMP-1 expression was also associated with reduced cell proliferation and identified as an independent factor associated with favorable patient outcomes. As IHC analysis revealed that MMP-1 is expressed at the tumor surface, but not at the cancer invasive front, the invasion-promoting ability of this enzyme may not be exhibited in GC tissues. However the present study may not have completely elucidated the precise mechanism by which Low MMP-1 expression contributed to increasing malignant potential in GC. In the future, an *in silico* analysis on the Cancer Genome Atlas data for GC patients may be required to evaluate implication of MMP-1 expression in GC progression. Taking the findings of the present study together, MMP-1 may act as a tumor suppressor in GC, although it is generally known to promote invasion in other cancer types. The assessment of MMP-1 expression in resected GC tissues may contribute to predicting cancer recurrence. If low MMP-1 expression is detected, postoperative chemotherapy may be considered, unless the cancer stage is low.

Acknowledgements

The authors would like to thank Dr Kazuyoshi Yanagihara (National Cancer Institute, Tokyo, Japan) for providing the GC cell line 58As9.

Funding

The present study was financially supported by JSPS KAKENHI Grant-in-Aid for Scientific Research (research project no. 18K08650).

Availability of data and materials

The datasets generated and/or analyzed during the current study are available from the corresponding author on reasonable request.

Authors' contributions

YK and KI conceived and designed the experiments. KI, KK, NE, HK, KO, KY and SM performed the experiments. YK, KI, TT and HN analyzed the data. KK contributed reagents, materials, or analytical tools. KI and YK wrote the paper.

KI and YK confirm the authenticity of all the raw data. All authors reviewed and approved the final manuscript.

Ethics approval and consent to participate

Informed consent to use the tissue specimens was obtained from each patient. The study was approved by the Ethics Committee of Saga University, Faculty of Medicine (approval no. 2020-10-R-03) and performed in accordance with the Declaration of Helsinki and current ethical guidelines. All animal protocols were approved by the Animal Care Committee of Saga University (approval no. A2020-015-0).

Patient consent for publication

Not applicable.

Competing interests

The authors declare that they have no competing interests.

References

- Smyth EC, Nilsson M, Grabsch HI, van Grieken NC and Lordick F: Gastric cancer. *Lancet* 396: 635-648, 2020.
- Karimi P, Islami F, Anandasabapathy S, Freedman ND and Kamangar F: Gastric cancer: Descriptive epidemiology, risk factors, screening, and prevention. *Cancer Epidemiol Biomarkers Prev* 23: 700-713, 2014.
- Harris AL: Hypoxia-a key regulatory factor in tumour growth. *Nat Rev Cancer* 2: 38-47, 2002.
- Lu X and Kang Y: Hypoxia and hypoxia-inducible factors: Master regulators of metastasis. *Clin Cancer Res* 16: 5928-5935, 2010.
- Poellinger L and Johnson RS: HIF-1 and hypoxic response: The plot thickens. *Curr Opin Genet Dev* 14: 81-85, 2004.
- Majmudar AJ, Wong WJ and Simon MC: Hypoxia-inducible factors and the response to hypoxic stress. *Mol Cell* 40: 294-309, 2010.
- Semenza GL, Jiang BH, Leung SW, Passantino R, Concordet JP, Maire P and Giallongo A: Hypoxia response elements in the aldolase A, enolase 1, and lactate dehydrogenase A gene promoters contain essential binding sites for hypoxia-inducible factor 1. *J Biol Chem* 271: 32529-32537, 1996.
- Comerford KM, Wallace TJ, Karhausen J, Louis NA, Montalto MC and Colgan SP: Hypoxia-inducible factor-1-dependent regulation of the multidrug resistance (MDR1) gene. *Cancer Res* 62: 3387-3394, 2002.
- Ide T, Kitajima Y, Miyoshi A, Ohtsuka T, Mitsuno M, Ohtaka K, Koga Y and Miyazaki K: Tumor-stromal cell interaction under hypoxia increases the invasiveness of pancreatic cancer cells through the hepatocyte growth factor/c-Met pathway. *Int J Cancer* 119: 2750-2759, 2006.
- Hara S, Nakashiro K, Klosek SK, Ishikawa T, Shintani S and Hamakawa H: Hypoxia enhances c-Met/HGF receptor expression and signaling by activating HIF-1 α in human salivary gland cancer cells. *Oral Oncol* 42: 593-598, 2006.
- Forsythe JA, Jiang BH, Iyer NV, Agani F, Leung SW, Koos RD and Semenza GL: Activation of vascular endothelial growth factor gene transcription by hypoxia-inducible factor 1. *Mol Cell Biol* 16: 4604-4613, 1996.
- Stoeltzing O, McCarty MF, Wey JS, Fan F, Liu W, Belcheva A, Bucana CD, Semenza GL and Ellis LM: Role of hypoxia-inducible factor 1 α in gastric cancer cell growth, angiogenesis, and vessel maturation. *J Natl Cancer Inst* 96: 946-956, 2004.
- Vaupel P, Mayer A and Höckel M: Tumor hypoxia and malignant progression. *Methods Enzymol* 381: 335-354, 2004.
- Kitajima Y and Miyazaki K: The critical impact of HIF-1 α on gastric cancer biology. *Cancers (Basel)* 5: 15-26, 2013.
- Rankin EB and Giaccia AJ: Hypoxic control of metastasis. *Science* 352: 175-180, 2016.
- Semenza GL: Targeting HIF-1 for cancer therapy. *Nat Rev Cancer* 3: 721-732, 2003.
- Singh D, Srivastava SK, Chaudhuri TK and Upadhyay G: Multifaceted role of matrix metalloproteinases (MMPs). *Front Mol Biosci* 2: 19, 2015.
- Brown PD: Matrix metalloproteinases in gastrointestinal cancer. *Gut* 43: 161-163, 1998.
- Gialeli C, Theocharis AD and Karamanos NK: Roles of matrix metalloproteinases in cancer progression and their pharmacological targeting. *FEBS J* 278: 16-27, 2011.
- Page-McCaw A, Ewald AJ and Werb Z: Matrix metalloproteinases and the regulation of tissue remodelling. *Nat Rev Mol Cell Biol* 8: 221-233, 2007.
- McCawley LJ and Matrisian LM: Matrix metalloproteinases: They're not just for matrix anymore! *Curr Opin Cell Biol* 13: 534-540, 2001.
- Boire A, Covic L, Agarwal A, Jacques S, Sherif S and Kuliopulos A: PAR1 is a matrix metalloproteinase-1 receptor that promotes invasion and tumorigenesis of breast cancer cells. *Cell* 120: 303-313, 2005.
- Shintani T, Kusuhara Y, Daizumoto K, Dondoo TO, Yamamoto H, Mori H, Fukawa T, Nakatsuji H, Fukumori T, Takahashi M and Kanayama H: The involvement of hepatocyte growth factor-MET-matrix metalloproteinase 1 signaling in bladder cancer invasiveness and proliferation. Effect of the MET inhibitor, cabozantinib (XL184), on bladder cancer cells. *Urology* 101: 169.e7-169.e13, 2017.
- Wang J, Liu D, Zhou W, Wang M, Xia W and Tang Q: Prognostic value of matrix metalloproteinase-1/protease-activated receptor-1 axis in patients with prostate cancer. *Med Oncol* 31: 968, 2014.
- Wang QM, Lv L, Tang Y, Zhang L and Wang LF: MMP-1 is overexpressed in triple-negative breast cancer tissues and the knockdown of MMP-1 expression inhibits tumor cell malignant behaviors in vitro. *Oncol Lett* 17: 1732-1740, 2019.
- Yamamoto H, Itoh F, Iku S, Adachi Y, Fukushima H, Sasaki S, Mukaiya M, Hirata K and Imai K: Expression of matrix metalloproteinases and tissue inhibitors of metalloproteinases in human pancreatic adenocarcinomas: Clinicopathologic and prognostic significance of matrilysin expression. *J Clin Oncol* 19: 1118-1127, 2001.
- Pittayapruek P, Meephansan J, Prapapan O, Komine M and Ohtsuki M: Role of matrix metalloproteinases in photoaging and photocarcinogenesis. *Int J Mol Sci* 17: 868, 2016.
- Wang K, Zheng J, Yu J, Wu Y, Guo J, Xu Z and Sun X: Knockdown of MMP-1 inhibits the progression of colorectal cancer by suppressing the PI3K/Akt/c-myc signaling pathway and EMT. *Oncol Rep* 43: 1103-1112, 2020.
- Grimm M, Lazariotou M, Kircher S, Stuermer L, Reiber C, Höfelmayr A, Gattenlöhner S, Otto C, Germer CT and von Rahden BH: MMP-1 is a (pre-)invasive factor in Barrett-associated esophageal adenocarcinomas and is associated with positive lymph node status. *J Transl Med* 8: 99, 2010.
- Eiró N, González LO, Atienza S, González-Quintana JM, Beridze N, Fernandez-Garcia B, Pérez-Fernández R, García-Caballero T, Schneider J and Vizoso FJ: Prediction of metastatic breast cancer in non-sentinel lymph nodes based on metalloproteinase-1 expression by the sentinel lymph node. *Eur J Cancer* 49: 1009-1017, 2013.
- Bianco BC, Scotti FM, Vieira DS, Biz MT, Castro RG and Modolo F: Immunohistochemical expression of matrix metalloproteinase-1, matrix metalloproteinase-2 and matrix metalloproteinase-9, myofibroblasts and Ki-67 in actinic cheilitis and lip squamous cell carcinoma. *Int J Exp Pathol* 96: 311-318, 2015.
- Hanrahan K, O'Neill A, Prencipe M, Bugler J, Murphy L, Fabre A, Pühr M, Culig Z, Murphy K and Watson RW: The role of epithelial-mesenchymal transition drivers ZEB1 and ZEB2 in mediating docetaxel-resistant prostate cancer. *Mol Oncol* 11: 251-265, 2017.
- Lassig AAD, Joseph AM, Lindgren BR and Yueh B: Association of oral cavity and oropharyngeal cancer biomarkers in surgical drain fluid with patient outcomes. *JAMA Otolaryngol Head Neck Surg* 143: 670-678, 2017.
- Kim M, Kim HJ, Choi BY, Kim JH, Song KS, Noh SM, Kim JC, Han DS, Kim SY and Kim YS: Identification of potential serum biomarkers for gastric cancer by a novel computational method, multiple normal tissues corrected differential analysis. *Clin Chim Acta* 413: 428-433, 2012.
- Altadill A, Rodriguez M, Gonzalez LO, Junquera S, Corte MD, González-Dieguez ML, Linares A, Barbón E, Fresno-Forcelledo M, Rodrigo L and Vizoso FJ: Liver expression of matrix metalloproteinases and their inhibitors in hepatocellular carcinoma. *Dig Liver Dis* 41: 740-748, 2009.

36. Du X, Wang S, Lu J, Cao Y, Song N, Yang T, Dong R, Zang L, Yang Y, Wu T and Li J: Correlation between MMP1-PAR1 axis and clinical outcome of primary gallbladder carcinoma. *Jpn J Clin Oncol* 41: 1086-1093, 2011.
37. Mizrahi A, Koren R, Hadar T, Yaniv E, Morgenstern S and Shvero J: Expression of MMP-1 in invasive well-differentiated thyroid carcinoma. *Eur Arch Otorhinolaryngol* 268: 131-135, 2011.
38. Ozden F, Saygin C, Uzunaslán D, Onal B, Durak H and Aki H: Expression of MMP-1, MMP-9 and TIMP-2 in prostate carcinoma and their influence on prognosis and survival. *J Cancer Res Clin Oncol* 139: 1373-1382, 2013.
39. Murray GI, Duncan ME, O'Neil P, McKay JA, Melvin WT and Fothergill JE: Matrix metalloproteinase-1 is associated with poor prognosis in oesophageal cancer. *J Pathol* 185: 256-261, 1998.
40. Murray GI, Duncan ME, O'Neil P, Melvin WT and Fothergill JE: Matrix metalloproteinase-1 is associated with poor prognosis in colorectal cancer. *Nat Med* 2: 461-462, 1996.
41. Inoue T, Yashiro M, Nishimura S, Maeda K, Sawada T, Ogawa Y, Sowa M and Chung KH: Matrix metalloproteinase-1 expression is a prognostic factor for patients with advanced gastric cancer. *Int J Mol Med* 4: 73-77, 1999.
42. Wang J, Ye C, Lu D, Chen Y, Jia Y, Ying X, Xiong H, Zhao W, Zhou J and Wang L: Matrix metalloproteinase-1 expression in breast carcinoma: A marker for unfavorable prognosis. *Oncotarget* 8: 91379-91390, 2017.
43. Liu M, Hu Y, Zhang MF, Luo KJ, Xie XY, Wen J, Fu JH and Yang H: MMP1 promotes tumor growth and metastasis in esophageal squamous cell carcinoma. *Cancer Lett* 377: 97-104, 2016.
44. Langenskiöld M, Ivarsson ML, Holmdahl L, Falk P, Kåbjörn-Gustafsson C and Angenete E: Intestinal mucosal MMP-1-a prognostic factor in colon cancer. *Scand J Gastroenterol* 48: 563-569, 2013.
45. Fujimoto D, Hirono Y, Goi T, Katayama K and Yamaguchi A: Prognostic value of protease-activated receptor-1 (PAR-1) and matrix metalloproteinase-1 (MMP-1) in gastric cancer. *Anticancer Res* 28: 847-854, 2008.
46. Tanaka T, Kitajima Y, Miyake S, Yanagihara K, Hara H, Nishijima-Matsunobu A, Baba K, Shida M, Wakiyama K, Nakamura J and Noshiro H: The apoptotic effect of HIF-1 α inhibition combined with glucose plus insulin treatment on gastric cancer under hypoxic conditions. *PLoS One* 10: e0137257, 2015.
47. Livak KJ and Schmittgen TD: Analysis of relative gene expression data using real-time quantitative PCR and the 2(-Delta Delta C(T)) method. *Methods* 25: 402-408, 2001.
48. Karlsson R, Pedersen ED, Wang Z and Brakebusch C: Rho GTPase function in tumorigenesis. *Biochim Biophys Acta* 1796: 91-98, 2009.
49. Martin DN, Boersma BJ, Yi M, Reimers M, Howe TM, Yfantis HG, Tsai YC, Williams EH, Lee DH, Stephens RM, *et al*: Differences in the tumor microenvironment between African-American and European-American breast cancer patients. *PLoS One* 4: e4531, 2009.
50. Hu C, Zhou H, Liu Y, Huang J, Liu W, Zhang Q, Tang Q, Sheng F, Li G and Zhang R: ROCK1 promotes migration and invasion of non-small-cell lung cancer cells through the PTEN/PI3K/FAK pathway. *Int J Oncol* 55: 833-844, 2019.
51. Fei F, Qu J, Zhang M, Li Y and Zhang S: S100A4 in cancer progression and metastasis: A systematic review. *Oncotarget* 8: 73219-73239, 2017.
52. Cho JY, Chung HC, Noh SH, Roh JK, Min JS and Kim BS: High level of urokinase-type plasminogen activator is a new prognostic marker in patients with gastric carcinoma. *Cancer* 79: 878-883, 1997.
53. Zheng HC, Sun JM, Li XH, Yang XF, Zhang YC and Xin Y: Role of PTEN and MMP-7 expression in growth, invasion, metastasis and angiogenesis of gastric carcinoma. *Pathol Int* 53: 659-666, 2003.
54. Valacca C, Tassone E and Mignatti P: TIMP-2 Interaction with MT1-MMP Activates the AKT Pathway and protects tumor cells from apoptosis. *PLoS One* 10: e0136797, 2015.
55. Pasquini G and Giaccone G: C-MET inhibitors for advanced non-small cell lung cancer. *Expert Opin Investig Drugs* 27: 363-375, 2018.
56. Wen B, Xu LY and Li EM: LOXL2 in cancer: Regulation, downstream effectors and novel roles. *Biochim Biophys Acta Rev Cancer* 1874: 188435, 2020.
57. Poplineau M, Schnekenburger M, Dufer J, Kosciarz A, Brassart-Pasco S, Antonicelli F, Diederich M and Trussardi-Régnier A: The DNA hypomethylating agent, 5-aza-2'-deoxycytidine, enhances tumor cell invasion through a transcription-dependent modulation of MMP-1 expression in human fibrosarcoma cells. *Mol Carcinog* 54: 24-34, 2015.
58. Poplineau M, Dufer J, Antonicelli F and Trussardi-Regnier A: Epigenetic regulation of proMMP-1 expression in the HT1080 human fibrosarcoma cell line. *Int J Oncol* 38: 1713-1718, 2011.
59. Zhang T, Fan J, Wu K, Zeng J, Sun K, Guan Z, Wang X, Hiesh JT and He D: Roles of HIF-1 α in a novel optical orthotopic spontaneous metastatic bladder cancer animal model. *Urol Oncol* 30: 928-935, 2012.
60. Zhou ZH, Ji CD, Xiao HL, Zhao HB, Cui YH and Bian XW: Reorganized Collagen in the tumor microenvironment of gastric cancer and its association with prognosis. *J Cancer* 8: 1466-1476, 2017.
61. Yin Y, Zhao Y, Li AQ and Si JM: Collagen: A possible prediction mark for gastric cancer. *Med Hypotheses* 72: 163-165, 2009.
62. Gao SY, Li J, Qu XY, Zhu N and Ji YB: Downregulation of Cdk1 and cyclinB1 expression contributes to oridonin-induced cell cycle arrest at G2/M phase and growth inhibition in SGC-7901 gastric cancer cells. *Asian Pac J Cancer Prev* 15: 6437-6441, 2014.
63. Kanthan R, Fried I, Rueckl T, Senger JL and Kanthan SC: Expression of cell cycle proteins in male breast carcinoma. *World J Surg Oncol* 8: 10, 2010.
64. Wang Y, Zhou X, Shan B, Han J, Wang F, Fan X, Lv Y, Chang L and Liu W: Downregulation of microRNA-33a promotes cyclin-dependent kinase 6, cyclin D1 and PIM1 expression and gastric cancer cell proliferation. *Mol Med Rep* 12: 6491-6500, 2015.
65. Liu FY, Wang LP, Wang Q, Han P, Zhuang WP, Li MJ and Yuan H: MiR-302b regulates cell cycles by targeting CDK2 via ERK signaling pathway in gastric cancer. *Cancer Med* 5: 2302-2313, 2016.
66. Chu DZ, Lang NP, Thompson C, Osteen PK and Westbrook KC: Peritoneal carcinomatosis in nongynecologic malignancy. A prospective study of prognostic factors. *Cancer* 63: 364-367, 1989.
67. Yonemura Y, Kawamura T, Bandou E, Tsukiyama G, Endou Y and Miura M: The natural history of free cancer cells in the peritoneal cavity. *Recent Results Cancer Res* 169: 11-23, 2007.
68. del Casar JM, Corte MD, Alvarez A, García I, Bongera M, González LO, García-Muñiz JL, Allende MT, Astudillo A and Vizoso FJ: Lymphatic and/or blood vessel invasion in gastric cancer: Relationship with clinicopathological parameters, biological factors and prognostic significance. *J Cancer Res Clin Oncol* 134: 153-161, 2008.
69. Kubo H, Kitajima Y, Kai K, Nakamura J, Miyake S, Yanagihara K, Morito K, Tanaka T, Shida M and Noshiro H: Regulation and clinical significance of the hypoxia-induced expression of ANGPTL4 in gastric cancer. *Oncol Lett* 11: 1026-1034, 2016.
70. Kosaka Y, Mimori K, Fukagawa T, Ishikawa K, Etoh T, Katai H, Sano T, Watanabe M, Sasako M and Mori M: Clinical significance of molecular detection of matrix metalloproteinase-1 in bone marrow and peripheral blood in patients with gastric cancer. *Ann Surg Oncol* 19 (Suppl 3): S430-S437, 2012.



This work is licensed under a Creative Commons Attribution-NonCommercial-NoDerivatives 4.0 International (CC BY-NC-ND 4.0) License.